

Failure Assessment Diagram for Titanium Brazed Joints

Yury Flom, Justin S. Jones, Mollie M. Powell, and David F. Puckett

The NASA STI Program Office ... in Profile

Since its founding, NASA has been dedicated to the advancement of aeronautics and space science. The NASA Scientific and Technical Information (STI) Program Office plays a key part in helping NASA maintain this important role.

The NASA STI Program Office is operated by Langley Research Center, the lead center for NASA's scientific and technical information. The NASA STI Program Office provides access to the NASA STI Database, the largest collection of aeronautical and space science STI in the world. The Program Office is also NASA's institutional mechanism for disseminating the results of its research and development activities. These results are published by NASA in the NASA STI Report Series, which includes the following report types:

- **TECHNICAL PUBLICATION.** Reports of completed research or a major significant phase of research that present the results of NASA programs and include extensive data or theoretical analysis. Includes compilations of significant scientific and technical data and information deemed to be of continuing reference value. NASA's counterpart of peer-reviewed formal professional papers but has less stringent limitations on manuscript length and extent of graphic presentations.
- **TECHNICAL MEMORANDUM.** Scientific and technical findings that are preliminary or of specialized interest, e.g., quick release reports, working papers, and bibliographies that contain minimal annotation. Does not contain extensive analysis.
- **CONTRACTOR REPORT.** Scientific and technical findings by NASA-sponsored contractors and grantees.

- **CONFERENCE PUBLICATION.** Collected papers from scientific and technical conferences, symposia, seminars, or other meetings sponsored or cosponsored by NASA.
- **SPECIAL PUBLICATION.** Scientific, technical, or historical information from NASA programs, projects, and mission, often concerned with subjects having substantial public interest.
- **TECHNICAL TRANSLATION.** English-language translations of foreign scientific and technical material pertinent to NASA's mission.

Specialized services that complement the STI Program Office's diverse offerings include creating custom thesauri, building customized databases, organizing and publishing research results . . . even providing videos.

For more information about the NASA STI Program Office, see the following:

- Access the NASA STI Program Home Page at <http://www.sti.nasa.gov/STI-homepage.html>
- E-mail your question via the Internet to help@sti.nasa.gov
- Fax your question to the NASA Access Help Desk at (443) 757-5803
- Telephone the NASA Access Help Desk at (443) 757-5802
- Write to:
NASA Access Help Desk
NASA Center for AeroSpace Information
7115 Standard Drive
Hanover, MD 21076



Failure Assessment Diagram for Titanium Brazed Joints

Yury Flom

Goddard Space Flight Center, Greenbelt, MD

Justin S. Jones

Goddard Space Flight Center, Greenbelt, MD

Mollie M. Powell

Goddard Space Flight Center, Greenbelt, MD

David F. Puckett

Goddard Space Flight Center, Greenbelt, MD

National Aeronautics and
Space Administration

Goddard Space Flight Center
Greenbelt, Maryland 20771

Trade names and trademarks are used in this report for identification only. Their usage does not constitute an official endorsement, either expressed or implied, by the National Aeronautics and Space Administration.

Available from:

NASA Center for AeroSpace Information
7115 Standard Drive
Hanover, MD 21076-1320

National Technical Information Service
5285 Port Royal Road
Springfield, VA 22161

FAILURE ASSESSMENT DIAGRAM FOR TITANIUM BRAZED JOINTS

ABSTRACT

The interaction equation was used to predict failure in Ti-4V-6Al joints brazed with Al 1100 filler metal. The joints used in this study were geometrically similar to the joints in the brazed beryllium metering structure considered for the ATLAS telescope. This study confirmed that the interaction equation $R_\sigma + R_\tau = 1$, where R_σ and R_τ are normal and shear stress ratios, can be used as conservative lower bound estimate of the failure criterion in ATLAS brazed joints as well as for construction of the Failure Assessment Diagram (FAD).

1.0 INTRODUCTION

The Ice, Cloud, and land Elevation Satellite-2 (ICESat-2) will use the Advanced Topographic Laser Altimeter System (ATLAS) to meet its scientific objectives. An integral part of the ATLAS instrument is the optical 532 nm telescope which is fabricated from beryllium. A structural element of the ATLAS telescope is a metering tower that provides support for the secondary mirror. The ICESat-2 program is considering brazing as a possible way of assembling the metering structure. When attempting to evaluate the load carrying capabilities of the beryllium brazed joints, it was realized that existing practices of structural analysis are lacking simple engineering methodology for estimating strength margins of brazed joints subjected to combined normal and shear stresses.

A study was initiated to develop a simple practice of conservative estimate of strength margins in the brazed joints. Due to the cost and health considerations, it was decided to perform this study on Ti/Al/Ti rather than Be/Al/Be system then apply the results of this study to other systems representing the flight applications.

Earlier work [1, 2] demonstrated that interaction equations could be used for failure assessment of the Albemet 162* joints brazed with AWS BAlSi-4 filler metal as well as stainless steel joints brazed with silver-based filler metals.

This memorandum provides a summary of work performed in this study and demonstrates that interaction equations used earlier could also be applied for failure assessment of Ti/Al/Ti brazed system.

*- Brush and Wellman trade name for 62%Be 38%Al metal matrix composite

2.0 APPROACH

A two part approach similar to [1] was also used in this study. In the first part, design values of tensile σ_o and shear τ_o strength (allowables) were determined. These allowables were used to construct interaction equation (1). The second part was performed to verify that this equation can be used as a lower bound FAD for Ti/Al/Ti brazed joints. A semi-empirical interaction equation proposed in [1,2] is shown below:

$$\frac{\sigma}{\sigma_o} + \frac{\tau}{\tau_o} \leq 1 \quad (1)$$

In this equation σ and τ are the maximum normal tensile and shear stresses acting on the filler metal layer within the brazed joint. σ_o and τ_o were determined experimentally. Equation (1) was validated by testing brazed T-specimens under combined tensile and shear loading configurations. Tensile and shear stresses acting on the brazed joints were calculated using the finite element analysis FeMAP program as well as engineering mechanics of materials equations (hand calculations), as described in the Appendix. An image-based strain measurement technique was employed during the mechanical tests to validate the results of the finite element analysis.

3.0 EXPERIMENTAL PROCEDURE

3.1 Test Specimens

Each specimen was given a unique identification to represent the test configuration. Test specimen identifications are explained in Table 1.

Table 1. Test Specimen Identification

Spec. ID	Example descriptions
B-1	Butt brazed specimen # 1
L1T1	Lap shear specimen # 1, nominal overlap length = 1T
L3T4	Lap shear specimen # 3, nominal overlap length = 4T
T-1	T-specimen # 1

All test specimens were fabricated from the Ti-6Al-4V alloy. Tensile and lap shear test specimens (Fig.1) were fabricated and tested to determine tensile and shear allowables. A T-specimen designed and fabricated to test the brazed joints under the combined action of shear and normal stresses is shown in Fig. 2.

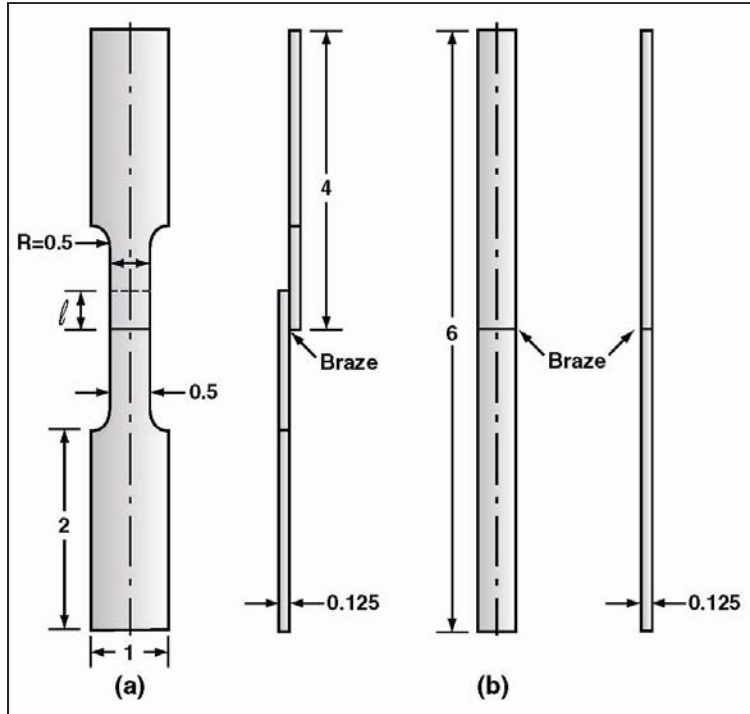


Fig.1 Lap shear (a) and butt tensile (b) specimens used in this effort to derive tensile and shear allowables. All dimensions are in inches.

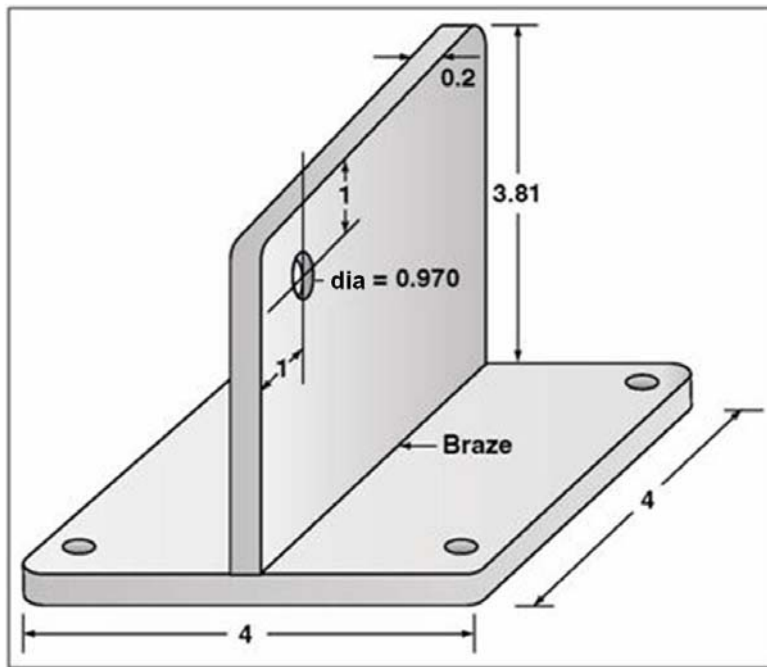


Fig. 2 T-specimens used for testing brazed joints under various loading configurations. Dimensions are in inches.

Brazing was performed in the vacuum furnace. All specimens were brazed with a 0.002 in (0.05 mm) foil of Al 1100 filler metal, preplaced between the faying surfaces of the braze joint prior to brazing. Typical time-temperature records of the brazing cycles are shown in Figure 3.

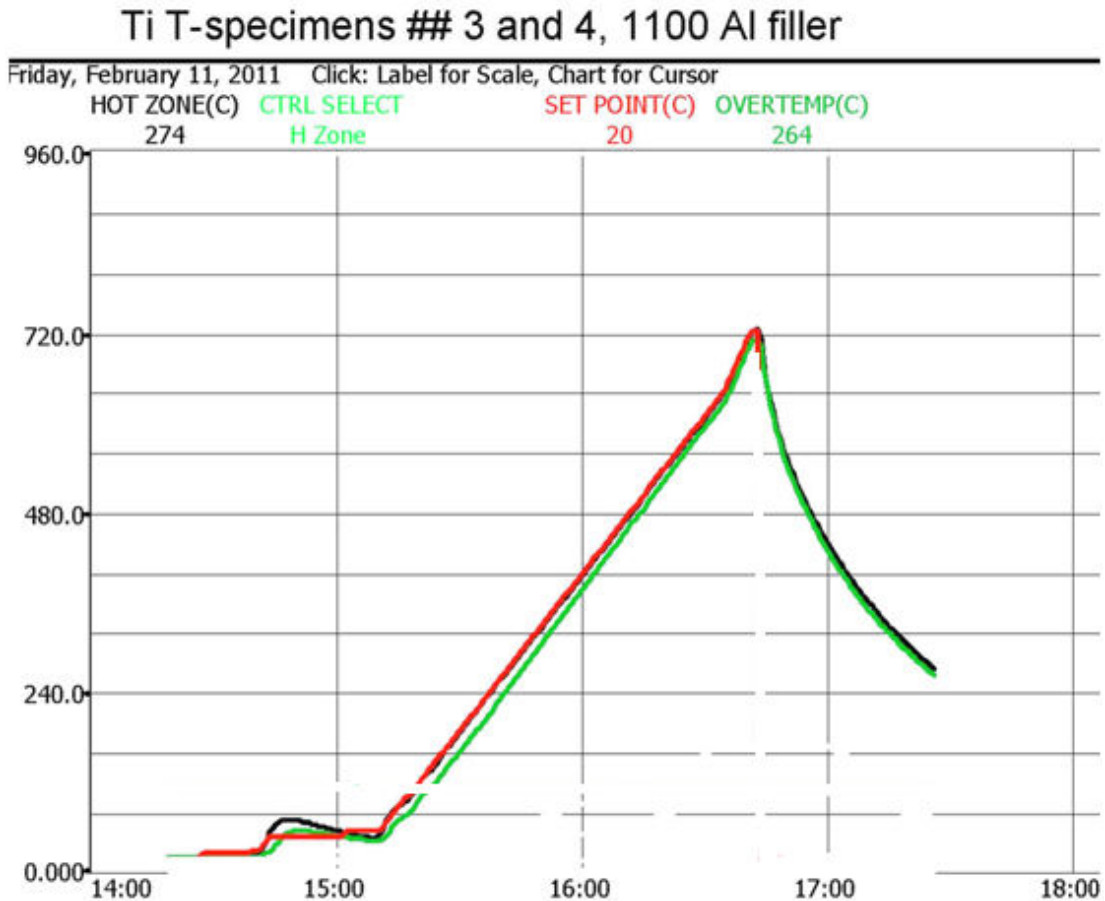


Fig.3 Time-temperature profile of the typical braze cycle

3.2 Mechanical testing

All specimens were tested on an Instron 4485 universal test frame. A total of six butt brazed specimens were tested. One specimen, marked B-6, had a noticeable misalignment and failed at a very low load. Consequently, it was considered an outlier and was ignored in estimating the tensile allowable. There were 4 groups of 3 lap shear specimens tested. Each group had the same nominal overlap length starting with 1T and ending with 4T, bringing a total number of lap shear specimens tested to 12. The purpose of testing various overlap lengths was to identify the lowest shear strength, as explained in more detail in [3].

The actual overlap length varied somewhat, since maintaining exact overlaps was not critical for the purpose of this investigation. Test results of the tensile tests are summarized in Table 2 while the results for the lap shear specimens are presented in Table 3.

Table 2 Butt Brazed Specimens Tensile Test Results

SPEC ID	MAX LOAD, lbs	AREA, in ²	TUS, ksi (MPa)	AVG TUS, ksi (MPa)	MIN TUS, ksi (MPa)	3 Sigma TUS,** ksi (MPa)
B1	1599	0.071	23 (155)	24 (166)	22 (153)	16 (110)
B2	1623	0.071	23 (158)			
B3	1573	0.071	22 (153)			
B4	2036	0.071	29 (198)			
B5	1791	0.071	25 (174)			
B6*	757	0.071	11 (74)			

*-Outlier; ** - 3 Sigma TUS = AVG – 3xSTDEV; STDEV = 2.7 ksi (18.6 MPa)

Table 3 Lap Shear Specimens Pull Test Results

SPEC. ID	MAX LOAD, lbs	OVERLAP, in	OVERLAP, T	WIDTH, in	AREA, in ²	SHEAR STRESS*, ksi	SHEAR STRESS, MPa
L1T1	1287	0.158	1.1	0.5	0.08	16.3	112.4
L2T1	1083	0.175	1.2	0.5	0.09	12.4	85.4
L3T1	1150	0.182	1.3	0.5	0.09	12.6	87.2
L1T2	1811	0.324	2.3	0.5	0.16	11.2	77.1
L2T2	1740	0.308	2.2	0.5	0.15	11.3	78.0
L3T2	1690	0.283	2.0	0.5	0.14	11.9	82.4
L1T3	2448	0.421	3.0	0.5	0.21	11.6	80.2
L2T3	2136	0.417	2.9	0.5	0.21	10.2	70.7
L3T3	2392	0.446	3.1	0.5	0.22	10.7	74.0
L1T4	3501	0.582	4.1	0.5	0.29	12.0	83.0
L2T4	3426	0.581	4.1	0.5	0.29	11.8	81.4
L3T4	3828	0.573	4.0	0.5	0.29	13.4	92.2

*- Shear stress calculated as maximum load divided by the overlap area.

In order to test T-specimens under combined tensile and shear loads, special 30° and 45° wedge fixtures were fabricated (see Fig. 4). By interchanging the different wedges and by varying the angle of rotation of the T-specimen, a total of 6 different loading configurations were established for this study, as indicated in Table 4.

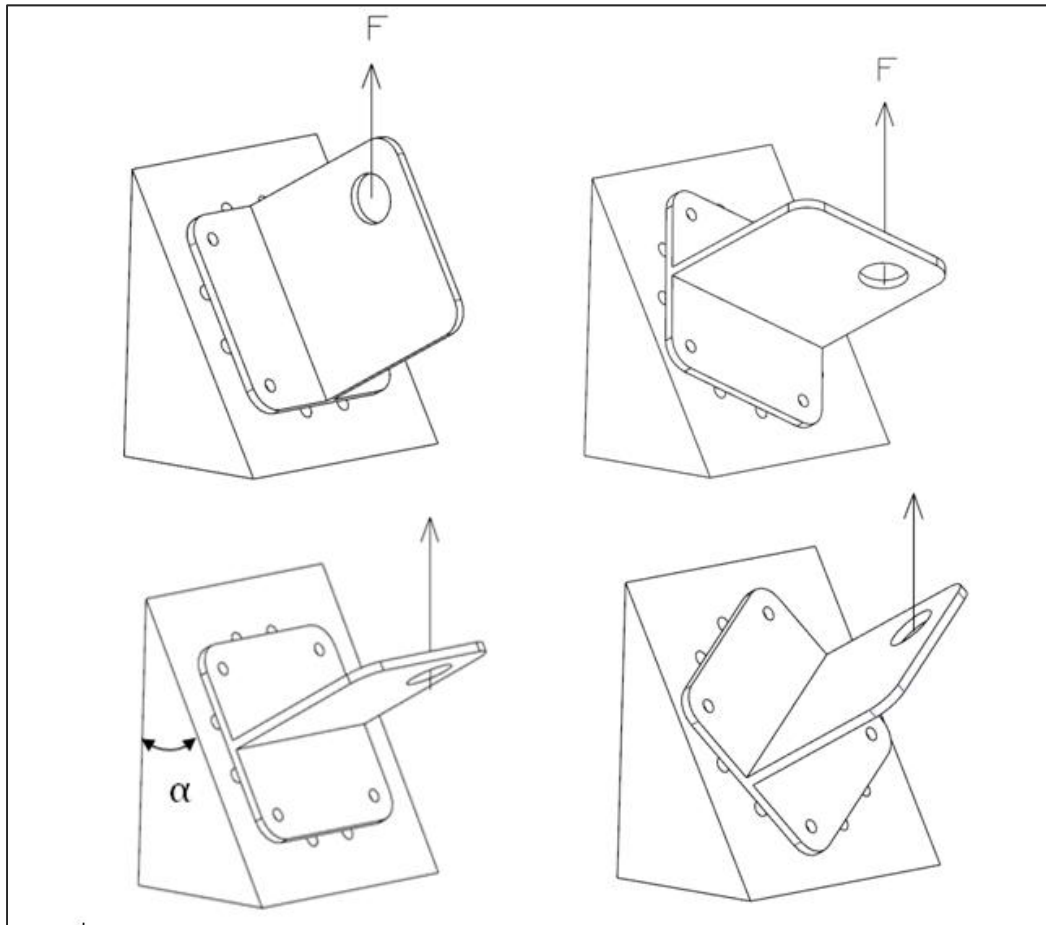


Fig.4. Different loading configurations of the brazed T-specimens. Wedge angle α was either 30° or 45° . Rotation of the T-specimen on the face of the wedge provided desired combined loading.

Table 4 T-specimens Test Results

ID	Loading case	Wedge angle, $^\circ$	Rotation angle, $^\circ$	Max Load F, lbs (kN)	Axial Components of F		
					Fx, lbs (kN)	Fy, lbs (kN)	Fz, lbs (kN)
T1	W45R0	45	0	3369 (15.0)	0	-2382 (-10.6)	2382 (10.6)
T2	W30R0	30	0	3649 (16.2)	0	-3160 (-14.1)	1825 (8.1)
T3*	W30R90	30	90	211 (0.9)	183 (0.8)	0	106 (0.5)
T4*	W30R60	30	60	328 (1.5)	246 (1.1)	-142 (-0.6)	164 (0.7)
T5	W30R90	30	90	414 (1.8)	359 (1.6)	0	207 (0.9)
T6	W30R120	30	120	383 (1.7)	-287 (-1.3)	166 (0.7)	192 (0.9)
T7	W45R90	45	90	395 (1.8)	279 (1.2)	0	279 (1.2)
T8	W30R60	30	60	493 (2.2)	370 (1.6)	-213 (-0.9)	247 (1.1)

*- these two specimens had braze flaws

At least one T-specimen was tested in each configuration. Four out of sixteen original plates used for brazing the T-specimens came distorted. The distortion of the plates prohibited proper contact between the faying surfaces. Rather than discarding the plates, it was decided to go ahead and braze these four plates with the understanding that the resultant T-specimens may be flawed. These specimens became T-3 and T-4 and were tested in the W30R90 and W30R60 configurations, respectively. The rationale behind testing the flawed specimens was an opportunity to compare their load carrying capability against higher quality brazed joints. Consequently, each flawed T-specimen was tested along with a regular specimen in the same loading configuration.

The T-specimen deformation was measured using an Aramis™ digital image correlation (DIC) system. This system uses two cameras in stereo, combined with a software-based geometric calibration which measures the precise relative angles and focal distances of the cameras to provide three-dimensional displacement information, as shown in Fig.5. For any location within the calibrated volume (defined to be on the order of the sample dimensions) which is viewable from both cameras, the three-dimensional displacements and full-field strains from objects under load can be measured.

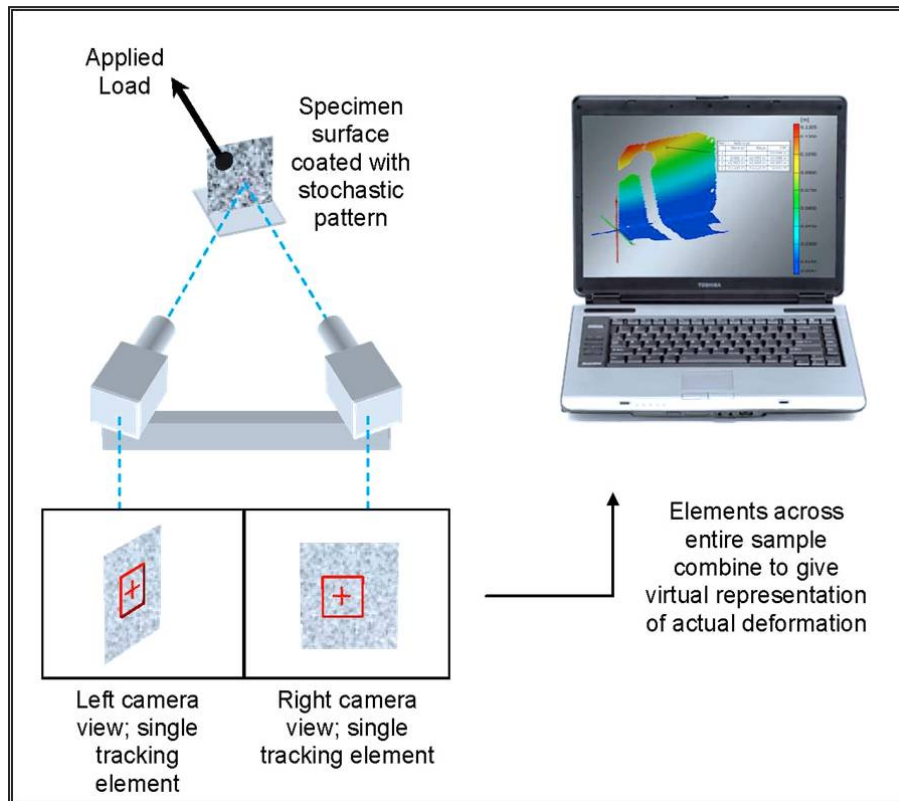


Fig.5 A schematic view of the ARAMIS™ DIC setup.

DIC measures strain by tracking the positions of identifiable features on the object's surface throughout the image sequence through the use of a virtual grid of markers which is superimposed onto the images within the software. While the measurement itself is non-destructive and non-invasive, DIC tracking is often aided by application of a stochastic speckle pattern or dry powder to the surface of the specimen which provides the locally unique, trackable features on the surface. For this study, the flat surfaces of the T-specimens were painted with a white background and a black speckle pattern, as shown in Fig.6

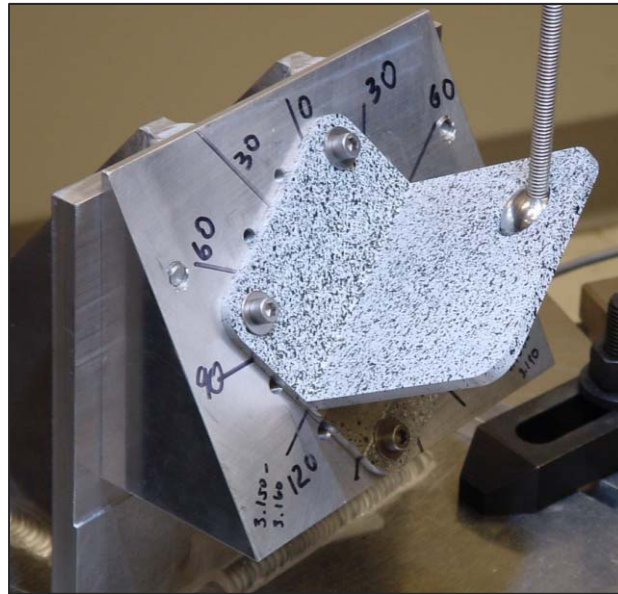


Fig. 6 Test setup showing the speckled T-specimen loaded into the test fixture.

During the test, the DIC system captured images at a rate of 0.5 Hz. Load data was also collected simultaneously through the Instron® load cell and was later correlated with the imaging data. The samples were loaded at a quasi-static, constant rate of displacement until failure.

3.3 Finite Element Analysis

Finite Element Analysis (FEA) of the T-specimens was performed using the engineering analysis software tool FeMap (Finite element Modeling and Post-processing). FeMap is sold by Siemens PLM Software and provides modeling tools as well as post processing capabilities. FeMap utilizes the engineering analysis software NX Nastran which is also distributed by Siemens. The global models were constructed using the dimensions from the actual test specimens (dimension can be found in Fig. 2 above). The global axis in relation to the specimen can be seen in Figure 7. This global axis was maintained

throughout all models and coincides with the global axis used by the DIC system. Each model was meshed with tetrahedral shaped elements at 0.24 inch in size.

Rigid body constraints were used to simulate the bolts holding the T-specimens to the wedge fixtures and were fixed in all directions and rotations. A rigid body was also used to simulate the ball fixture used to load the T-specimen. The center node of the rigid body was placed at the center location of the ball for each different T-specimen test configuration. The loading for each test configuration was then placed on this center node. The breaking load found during mechanical testing was used to analyze each model and to calculate the shear and tensile stresses within the braze joint. The FEA-calculated shear and tensile stresses were then compared to hand calculations. For added confidence, the deformation data obtained from FeMAP were compared to the deformation data provided by the DIC.

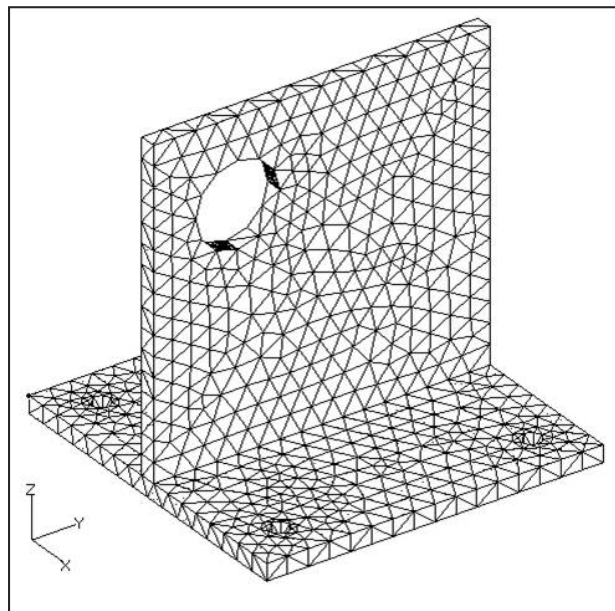


Fig.7 Global FEA model of T-specimen

4. RESULTS AND DISCUSSION

4.1 Mechanical Tests - Butt and Lap Shear Specimens

Tensile Ultimate Strength (TUS) of tested butt brazed specimens varied between 22 and 29 ksi (153 and 198 MPA), as shown in Table 2. The number of specimens was too small for a meaningful A- or B-basis statistical analysis; it was felt, however, that the number of the test specimens was sufficient for verifying the methodology.

Consequently, the tensile stress ratio can be determined using average, minimum, or the three sigma value of TUS given in Table 2, above.

Shear strength was measured on single lap shear specimens having different overlap lengths, as per AWS C3.2 [3]. The test results shown in Table 3 are plotted as a function of the overlap length in Fig.8. As one can see, the data generally follows the well-known experimental trend observed while testing numerous lap joints regardless of the joint geometries: as overlap length increases the average shear strength of the brazed joint decreases [4].

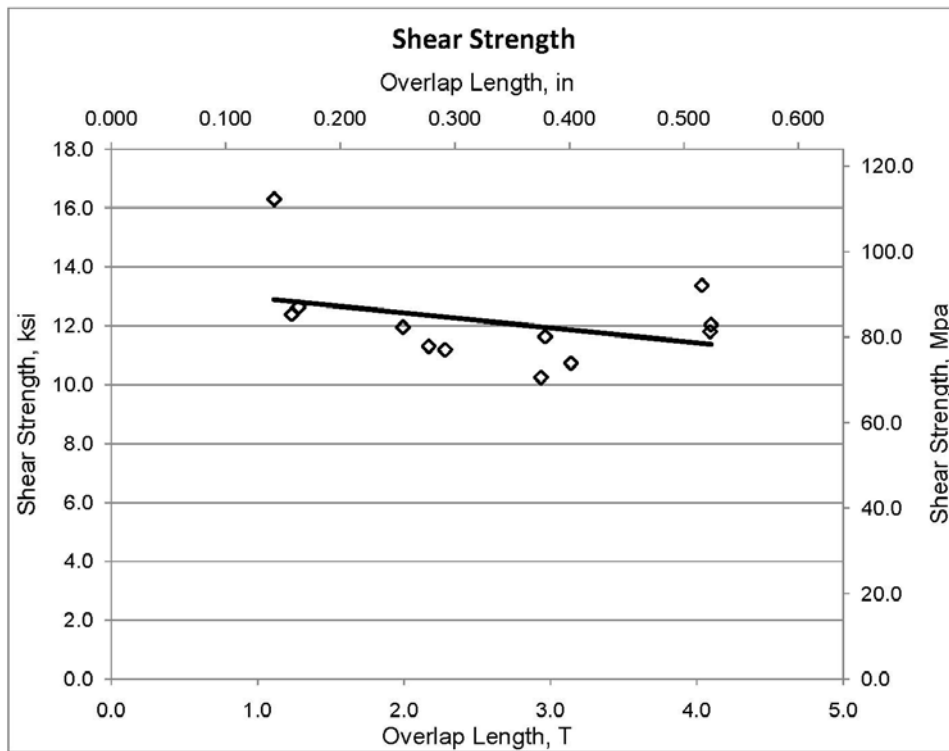


Fig.8 Plot of the lap shear test results vs. overlap length.

It is not completely clear why there is a slight increase in shear strength observed on the specimens with the longest overlap tested. Since the specimens with the same overlap were brazed in one batch, there could be a batch-to-batch variability in brazed joint strength. A slight overheating during brazing could result in reduction of the brazed joint strength causing an artificial “dip” in data shown in Fig. 8. This artifact, however, has very little impact on the present study. For the purpose of calculating the shear stress ratio, the lowest experimentally observed average shear strength of the lap shear specimens should be used in order to have a conservative estimate. The lowest shear strength observed in this study is about 10 ksi (70 MPa). This value is still higher than the 8 ksi (55 MPa) shear strength of 1100 Al reported elsewhere [5]. Therefore, the shear stress ratios can be determined using either 10 or 8 ksi (70 or 55 MPa). Value of 8 ksi was selected as more conservative.

4.2 Mechanical Tests – T-specimens

Results of mechanical testing of the T-specimens are shown in Table 4. As expected, the failure loads of the flawed specimens T3 and T4 were significantly less than the flaw-free specimens subjected to identical loading cases. Typical fracture surfaces of the T-specimen brazed joints are shown in Fig. 9. The total lack of braze area found in specimens T3 and T4 were estimated to be approximately 26% and 14%, respectively, based on a digital area threshold analysis of the cross-section.

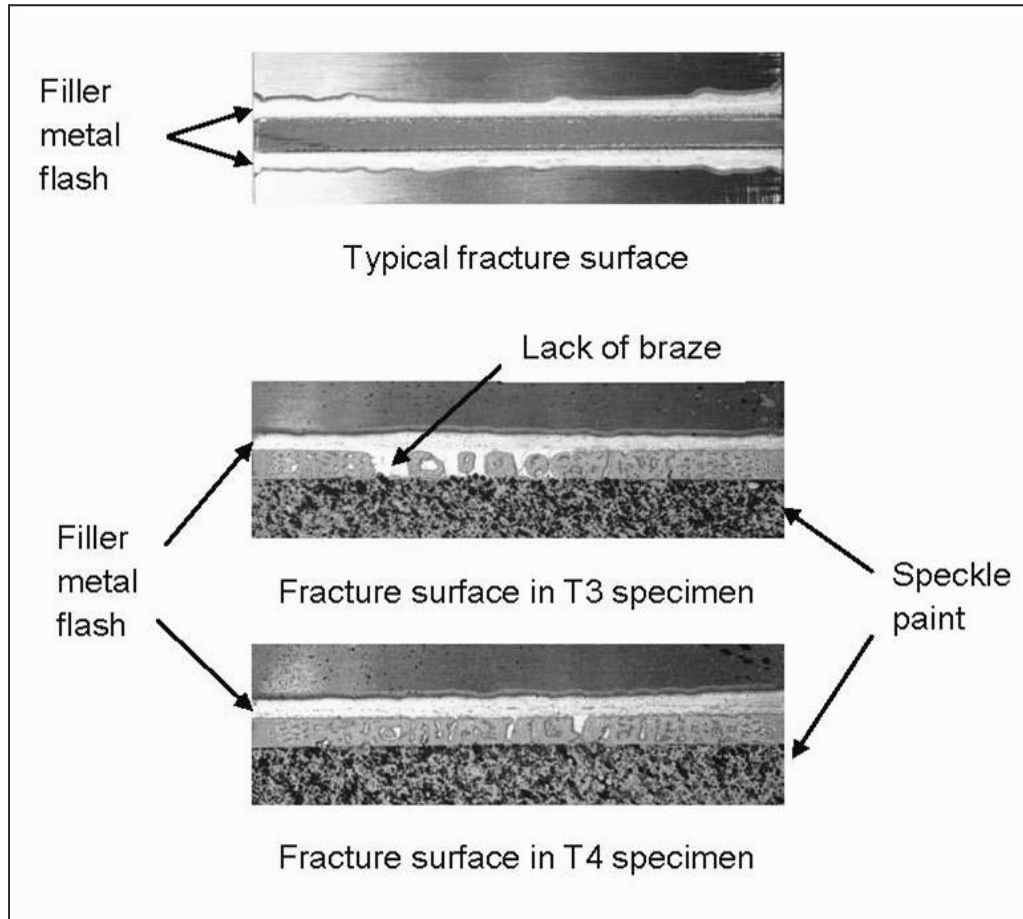


Fig.9 Typical fracture surfaces (top) of the fractured T-specimens showing the entire, end-to-end brazed joints. The lower images showed fracture surfaces containing lack of braze in T3 and T4 specimens. Horizontal plates containing the braze joint “foot print” were used to take these photographs.

Results of comparison between displacements obtained independently from FEA and DIC analysis are shown in Table 5. As one can see, total displacements at specific locations on the T-specimens at failure loads calculated by these two methods are within 2.5% for specimens T4 -T8.

Table 5 FEA vs. DIC Total Displacement Comparison

Method	T3	T4	T5	T6	T7	T8	T3 reduced	T4 reduced
FeMap, in	0.056	0.067	0.098	0.069	0.070	0.097	0.056	0.068
DIC, in	0.055	0.068	0.098	0.068	0.068	0.096	0.055	0.068
Difference, %	1.8	1.5	0.0	1.5	2.9	1.0	1.8	0.00

Such a good match gives high confidence that the FEA models and results are correct. Figure 10 shows images of the deformed T-specimens at failure generated by FEA and DIC.

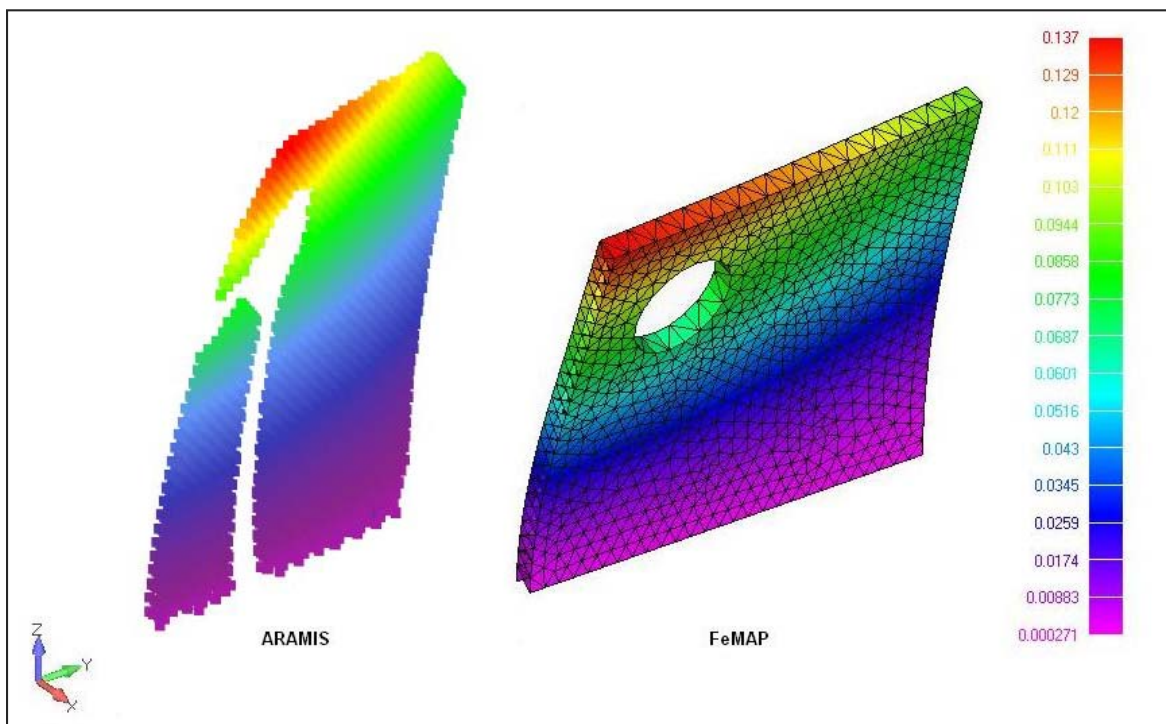


Fig.10 Images of the deformed T-specimens at failure generated by DIC and FEA.

Quite unexpected is a close agreement between FEA and DIC results for the flawed T3 and T4 specimens. Since initial FEA models for T3 and T4 specimens did not take into account reduction in braze area due to lack of braze (LOB), the only conclusion one can make is that the stiffness of the flawed T3 and T4 specimens was not affected by the lack of braze, even as high as 26%! Indeed, a comparison of the load vs. crosshead displacement records of T4 vs T8 and T3 vs.T5, as shown in Fig. 11, demonstrates a very small difference in stiffness between the flawed and non-flawed specimens.

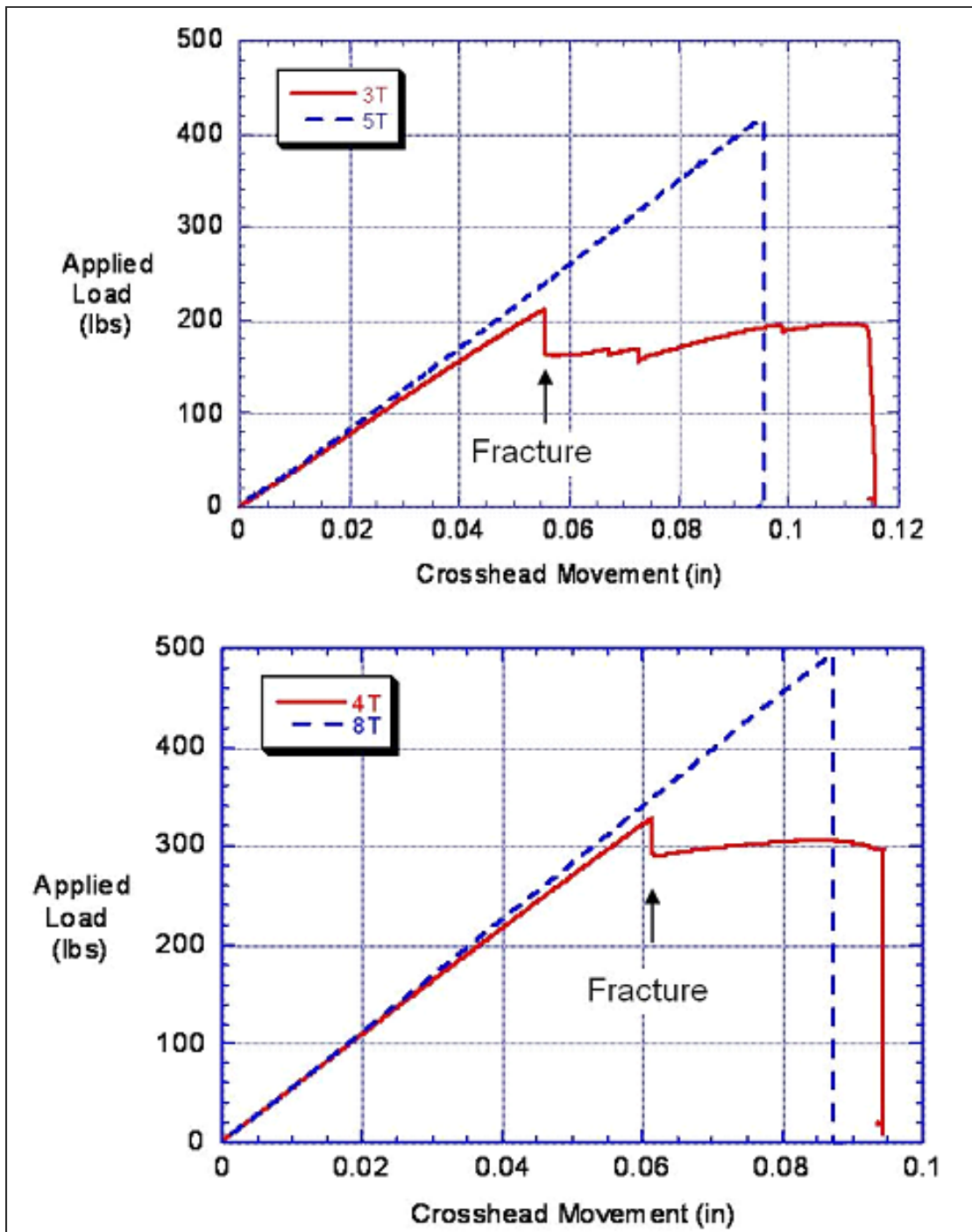


Fig.11 Tensile tests of the T3 and T4 brazed specimens containing flaws are compared with the flaw-free T5 and T8 specimens (dashed line) tested in identical loading configurations. Note a small difference in stiffness between the flawed and flaw-free specimens. Arrows indicate fracture of the flawed T3 and T4 specimens.

In an attempt to account for LOB in the finite element analysis, FEA models for T3 and T4 specimens were modified by reducing the braze area by 26% and 14% accordingly. This was accomplished by uniformly reducing the brazed joint width in the modified T3 and T4 FEA models, as shown in Fig.12.

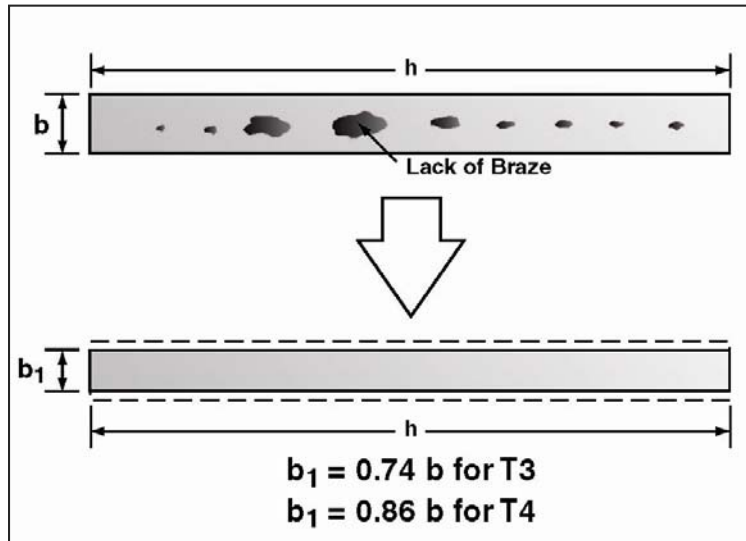


Fig.12 A schematic showing lack of braze modeled by simple reduction of the braze width from b to b_1

The FEA results can be found in Table 6; for the “reduced area”, T3 and T4 are denoted by T3 - reduced and T4 – reduced. For comparison, the results of hand calculations are provided in Table 7.

Table 6 FEA Results

Specimen ID	Failure Load (lb)	Max Princ (MPa)	Max Princ (ksi)	σ Ratio, R_σ	Max Shear (MPa)	Max Shear (ksi)	τ Ratio, R_τ
T1	3369	89	12.9	0.8	43	6.2	0.8
T2	3649	118	17.1	1.1	57	8.2	1.0
T3 (Flawed)	211	124	17.9	1.1	62	9.0	1.1
T4 (Flawed)	328	161	23.4	1.5	89	12.9	1.6
T5	414	243	35.2	2.2	121	17.6	2.2
T6	383	197	28.5	1.8	101	14.6	1.8
T7	395	197	28.6	1.8	99	14.3	1.8
T8	493	254	36.8	2.3	130	18.9	2.4
T3 reduced	211	253	36.6	2.3	133	19.3	2.4
T4 reduced	328	267	38.7	2.4	147	21.3	2.7

Table 7 Hand Calculated Principal Stresses and Stress Ratios

ID	Loading case	Failure load, (lbs)	σ_1 (ksi)	σ_1 (MPa)	τ_{max} (ksi)	τ_{max} , (MPa)	σ Ratio, R_σ	τ Ratio, R_τ
T1	W45R0	3369	12.6	87	7.1	49	0.8	0.9
T2	W30R0	3649	17.4	120	9.7	67	1.1	1.2
T3 (flawed)	W30R90	211	18.5	127	9.8	67	1.2	1.2
T4 (flawed)	W30R60	328	25.2	174	13.4	92	1.6	1.7
T5	W30R90	414	36.2	250	19.2	132	2.3	2.4
T6	W30R120	383	30.1	207	15.9	110	1.9	2.0
T7	W45R90	395	28.6	197	15.1	104	1.8	1.9
T8	W30R60	493	37.8	261	20.1	139	2.4	2.5

A good match between FEA and DIC displacements for the “reduced” specimens as well as closer proximity of failure stresses to their T5 and T8 counterparts indicate that the flawed T3 and T4 discontinuities can be reasonably well represented by the reduced area FEA models.

The data from Table 6 is plotted as normal stress vs. shear stress and as stress ratios in Figure 13 while the hand calculations are plotted in Figure 14. A combined plot representing the FEA and hand calculation results are shown in Fig. 15. As one can see there is a good agreement between FEA and hand calculated stress values and/or stress ratios. Stress ratios R_σ and R_τ were calculated as:

$$R_\sigma = \frac{\sigma_1}{\sigma_0} \text{ and } R_\tau = \frac{\tau_{max}}{\tau_0},$$

where σ_0 and τ_0 are 16 ksi (110 MPa) and 8 ksi (55 MPa) respectively.

For convenience, the results of lap shear and butt-brazed pull tests (Tables 2 and 3) are also plotted along their respective axis in Figures 13-15. Since the strength of the standard test specimens is typically reported in terms of the average values, determined as failure force divided by the total area of the brazed joint (3), the data points representing these specimens in Figures 13-15 are also based on average values.

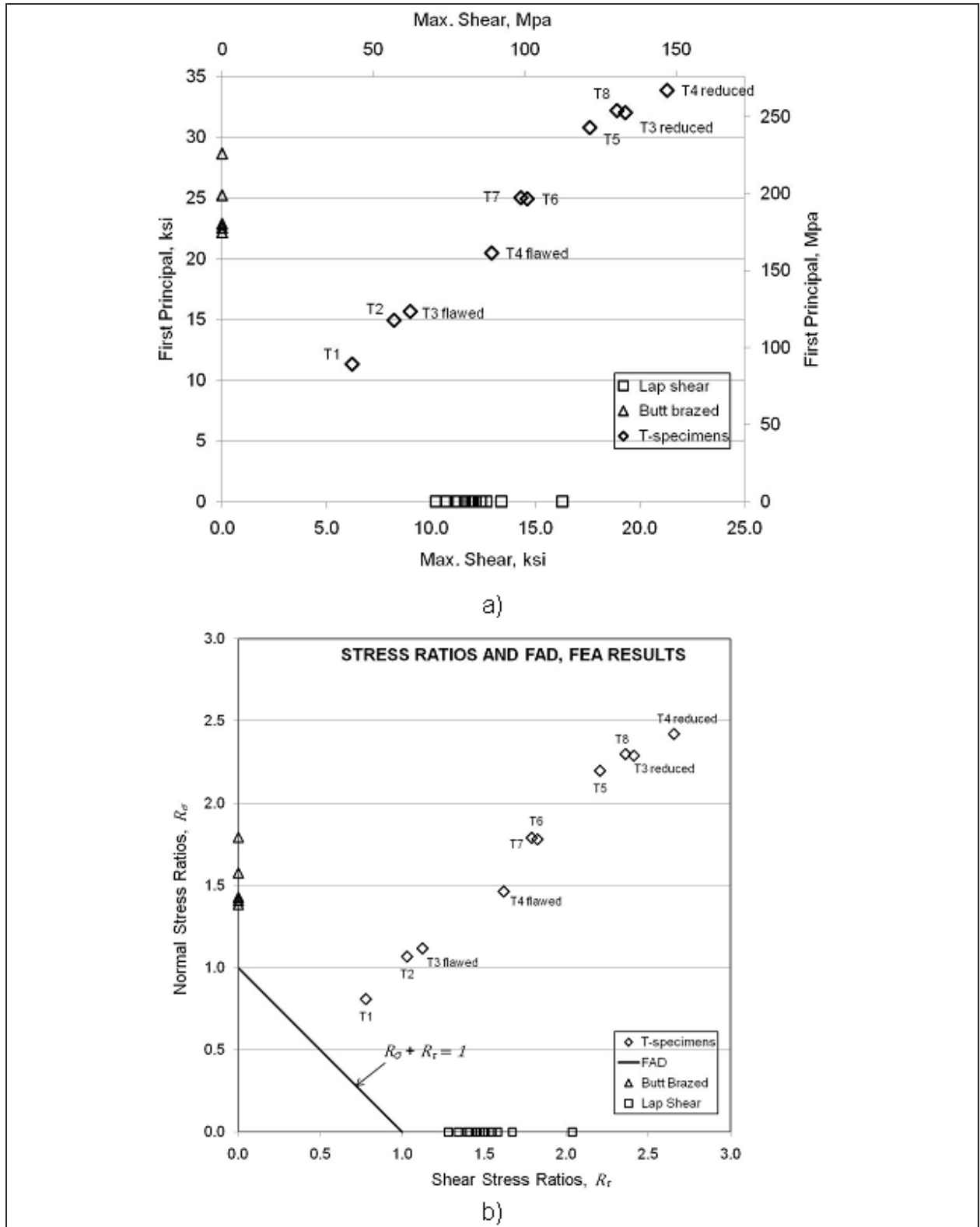
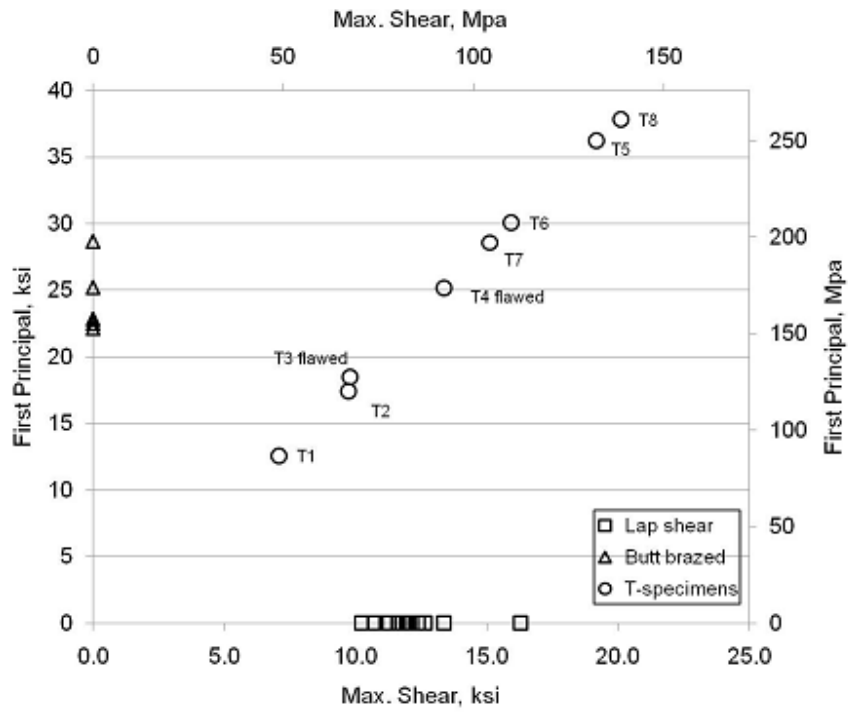
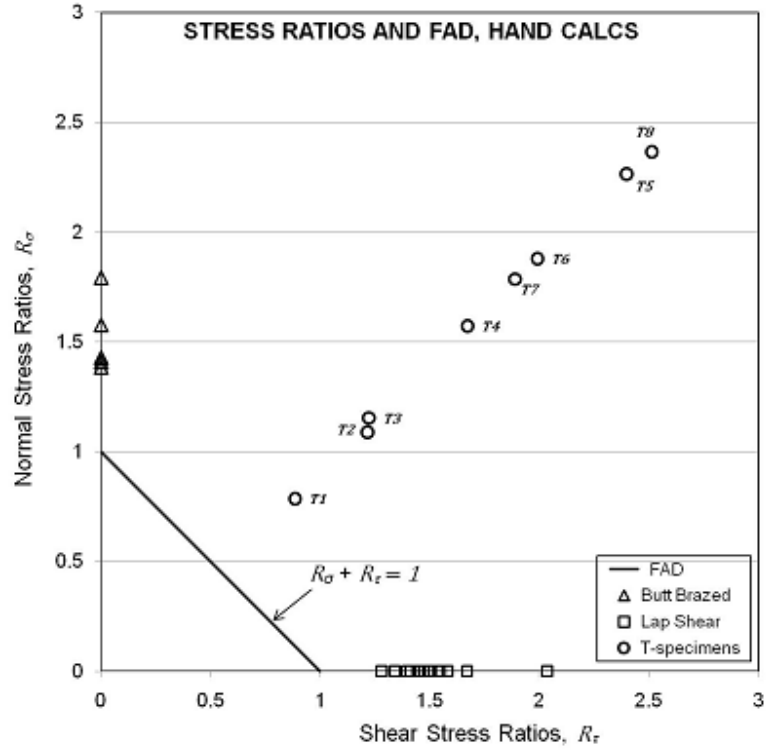


Fig.13 FEA results for T-specimens plotted as stresses (a) or stress ratios (b).



a)



b)

Fig.14 Hand calculated results for T-specimens plotted as stresses (a) and stress ratios (b).

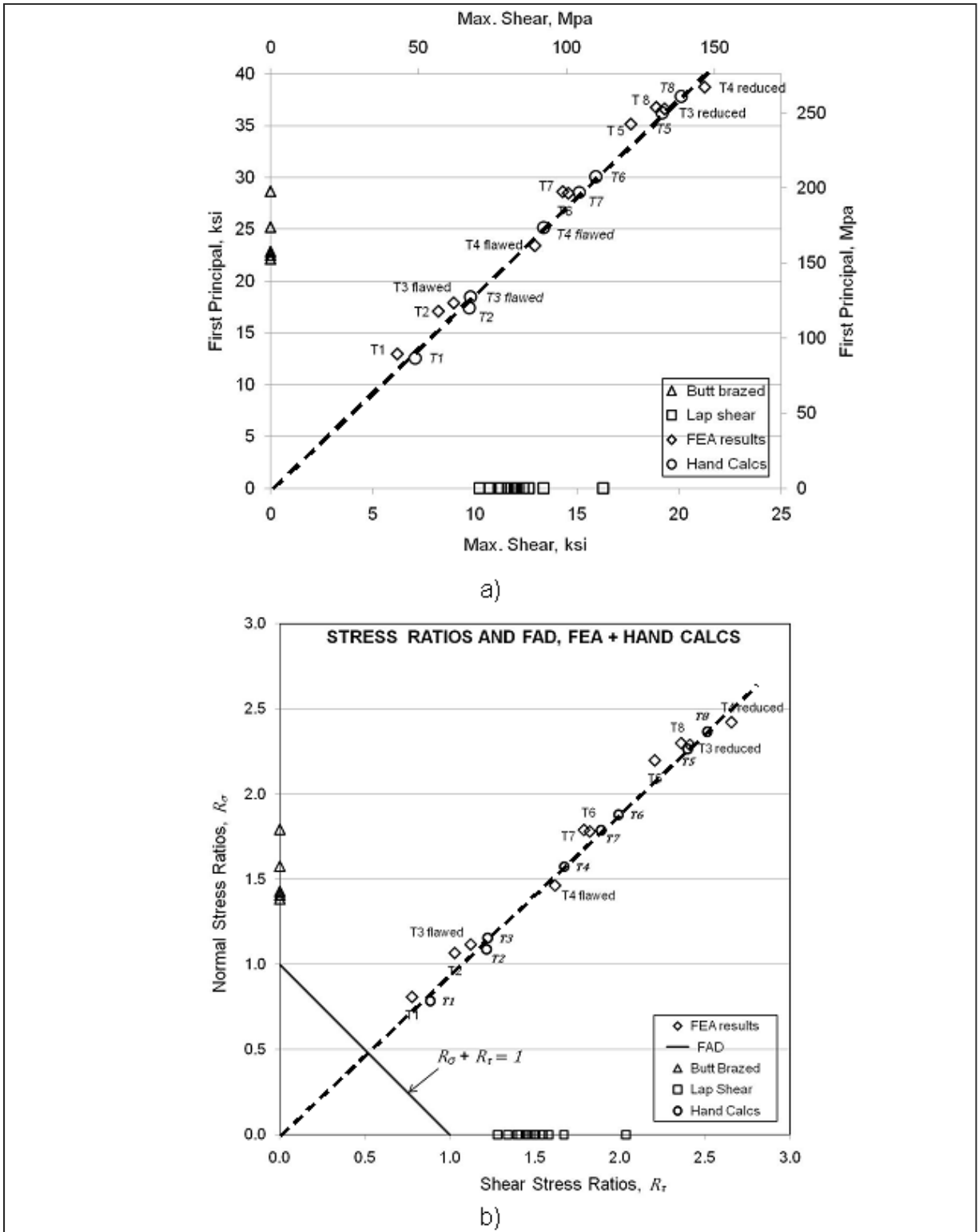


Fig. 15 Shows a good agreement between FEA and hand calculations plotted in terms of stresses (a) or stress ratios (a). Trend lines (dashed) are also shown for convenience

Several interesting observations can be made when examining the graphs in Figs.13 - 15.

- It appears that all T specimens subjected to combined normal, bending, shear and torsional loads, such as specimens T3 – T8, all fall on the same straight trend line emanating from the origin. This means that the ratio of maximum normal principal and maximum shear stresses remains the same regardless of the loading configurations.
- It appears that a relative position of the data point along the trend line is related to the strength or quality of the brazed joint. Note that specimens T8 and T4, as well as T5 and T3 were tested under identical loading configurations. The major difference between them, however, was the fact that brazed joints in T3 and T4 had 26 and 14% lack of braze. Consequently, these flawed specimens failed at significantly lower stresses while remaining on the same trend line.
- As one can see all the data points are located fairly far (even the flawed T3 and T4 specimens) from the Safe Zone. This indicates a fairly conservative selection of the FAD line.
- When the braze areas in the FEA models for T3 and T4 flawed specimens are reduced by 26 and 14%, the estimated failure stresses increase and move up along the same lines closer to the T5 and T8 specimens tested under loading configurations identical to T3 and T4 respectively. This indicates that lack-of-braze discontinuities (at least of the type observed in T3 and T4) can be reasonably modeled by reducing the total braze area.
- Since the trend line is a straight line radiating from the origin, only one point is necessary to define an angular position of such line. A position of such point on the plot can be established from FEA analysis of the actual brazed assembly using a global FEA model subjected to the design loading conditions.

Based on these observations, the following procedure of estimating margins of safety for brazed joints in a structure can be recommended:

1. determine tensile and shear allowables by testing standard brazed test specimens and construct FAD line;
2. using FEA determine 1st principal and max shear stresses acting on the braze plane in the actual structural brazed joint subjected to design loads;
3. connect the origin with the point determined in 2) and construct a trend or braze joint line;
4. an intercept of FAD line and the braze joint line corresponds to a zero safety margin condition;
5. fabricate a small number (two or three) of identical or “realistic” specimens representing actual brazed joint geometry and test them to failure under

identical loading conditions. This step will help to determine the actual normal and shear stresses causing failure and define the location of the failure point on the braze joint line. If the actual level of stresses causing failure is of no consequence, this step can be omitted

This procedure is illustrated graphically in Fig. 16.

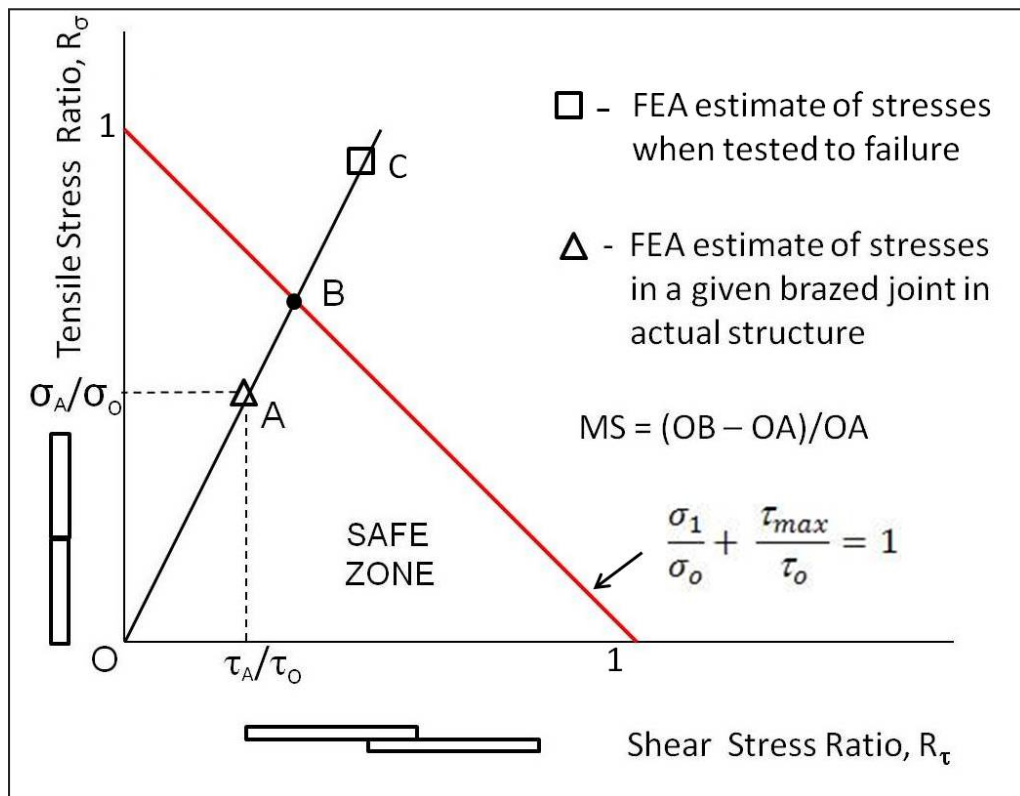


Fig. 16 Illustration of a structural evaluation of the brazed assembly. FAD is constructed based on experimental determination of shear τ_o and tensile σ_o allowables. Area inside the FAD line is a safe combination of stresses, or the safe zone. 1st principal and maximum shear in the brazed joint of interest subjected to the design loads are estimated by FEA using global model of the brazed assembly. Point A represents these stresses σ_A and τ_A normalized over their respective allowables. The trend or braze joint line is constructed by connecting O and A. Intercept of the braze joint line with FAD gives point B representing zero Margin of Safety (MS). MS is estimated as $(OB/OA) - 1$; Point C represents the actual stresses at failure estimated from testing of the “realistic” specimens representing the brazed joint geometry and loading conditions.

Since the data points corresponding to all T3 – T8 specimens are located on the same braze joint line, it would be logical to expect the data points representing failure conditions of these specimens to form a closely spaced cluster located on the braze joint line. However, as one can see, these data points are spread quite far apart, particular T1 and T8. It is plausible that one of the reasons for such scatter in the T specimens test data is the propagation of error effect. Since the test results for standard butt tensile and lap shear brazed specimens show considerable scatter, it is reasonable to expect no lesser scatter when testing the specimens under more complicated loading conditions. A rigorous statistical analysis of propagation of error is difficult to perform since the exact functional relationship between normal and shear stresses and actual failure criterion is not known. Another possible reason for such scatter is a different sensitivity of the brazed joints to various types of stresses.

5. CONCLUSIONS

1. The Failure Assessment Diagram (FAD) based on eq.(1) can provide a very conservative estimate of safe static load carrying capabilities of the brazed joints;
2. The applicability of FEA analysis to determine the 1st principal and maximum shear stresses for a complex loading geometry was validated using DIC analyzed experimental results.
3. Such conservatism is justified by a large scatter in mechanical properties of the brazed joints, even when determined by testing the standard test specimens;
4. A degree of conservatism of FAD can be controlled by the level of conservatism used to estimate brazed joint allowables. For example, A-basis allowables will result in the most conservative FAD;
5. It appears that safety margins of the brazed joints can be estimated by using the simple engineering procedure proposed in this study. More work is required to verify that this procedure is applicable for other base – filler metal brazed joint combinations and structures.

Acknowledgements

The authors would like to thank IceSAT 2 project for sponsoring this study. Many thanks also go to Sheila Wall, Séké Godo, Wayne Chen and Babak Farrokh (code 542) for their assistance with FEA and hand calculations.

Appendix

Normal and shear stresses acting on the braze plane in brazed joints were hand calculated using engineering mechanics [6,7]. Figure 17 illustrates the steps and nomenclature used to develop the necessary equations for normal and shear stresses. X, Y, and Z components of the applied force P can be calculated as:

$$\begin{aligned} P_x &= P \cdot \cos \theta \cdot \sin \varphi \\ P_y &= P \cdot \cos \theta \cdot \cos \varphi \\ P_z &= P \cdot \sin \theta \end{aligned}$$

First, for convenience, the point A where the test load is applied is relocated to the center of cross section, point B. To compensate for this relocation, three moments need to be introduced:

$$P_x \cdot (d_2), P_z \cdot (d_1) \text{ and } P_y \cdot (d_2)$$

Normal or axial stress on the braze plane is due to axial component P_z due to bending. The general form of the equation used to calculate normal stress acting at points 1 through 8 in the braze plane is:

$$\frac{P_z}{A} + \sum \frac{M \cdot c}{I}$$

Where $A=b \cdot h$ is the area of the brazed joint footprint. The second term, in this equation, is a sum of all bending stresses and c represents the distance to neutral axis for each of the bending stresses and equals either $h/2$ or $b/2$. For example, normal stress at point 1 can be calculated as:

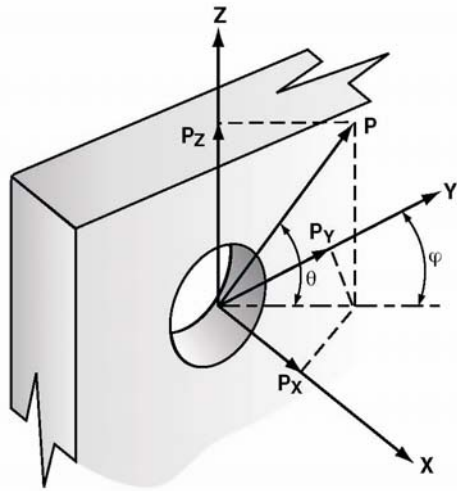
$$\sigma_z = \frac{P_z}{A} + \frac{-P_z \cdot d_1 \cdot \left(\frac{h}{2}\right)}{I_{xx}} + \frac{-P_x \cdot d_2 \cdot \left(\frac{b}{2}\right)}{I_{yy}} + \frac{-P_y \cdot d_2 \cdot \left(\frac{h}{2}\right)}{I_{xx}},$$

Where $I_{xx} = (b \cdot h^3)/12$ and $I_{yy} = (b^3 \cdot h)/12$ are moments of inertia. Shear stresses due to shear and torsion have their maximum values at mid-points of each side, such as points 2,5,7 and 8 (see Fig. 17). For example, a total shear stress at points 2 and 5 can be calculated as:

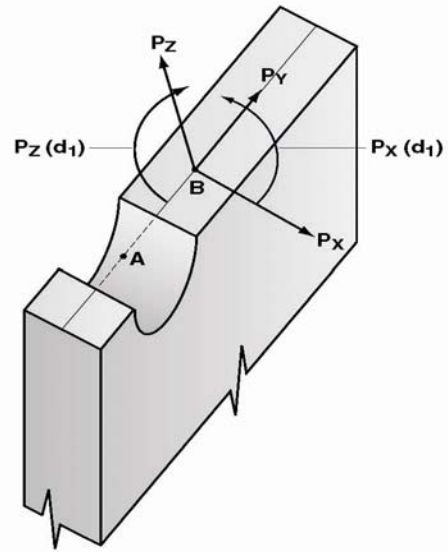
$$\tau_{xy} = \frac{1.5 \cdot P_y}{b \cdot h} + \frac{3 \cdot P_x \cdot (d_1)}{8 \cdot \left(\frac{h}{2}\right) \cdot \left(\frac{b}{2}\right)^2} \cdot \left[1 + 0.6095 \cdot \left(\frac{b}{h}\right) + 0.8865 \cdot \left(\frac{b}{h}\right)^2 - 1.8023 \cdot \left(\frac{b}{h}\right)^3 + 0.91 \cdot \left(\frac{b}{h}\right)^4 \right]$$

Shear stresses at mid-points 7 and 8 can be calculated as:

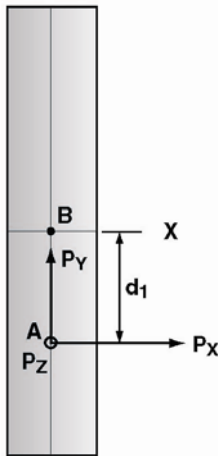
$$\tau = \frac{1.5 \cdot P_x}{b \cdot h}$$



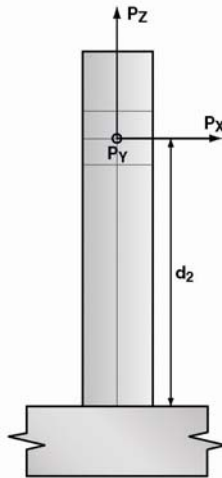
a)



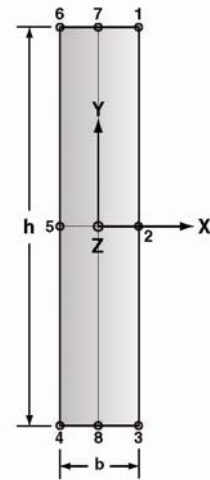
b)



c)



d)



e)

Fig. 17 Several sketches that help to better understand hand calculation process. Test load was applied in a direction represented by force P , as shown in sketch (a). The load components P_x , P_y and P_z are transferred to the center B and the new moments are introduced (b). Sketch (c) shows how torsion is developed in the braze plane due to component P_x acting over distance d_1 . Sketch (d) is a vertical cross section of the T-specimen showing bending moment $P_x \cdot d_2$. Finally, sketch (e) shows the braze plane and all locations where normal and shear stresses were calculated.

Results of hand calculations are shown in Table 6. Principal stresses and maximum shear stresses at each location 1 through 8 were calculated using the following expressions:

$$\sigma_1, \sigma_3 = \frac{\sigma_z}{2} \pm \sqrt{\left(\frac{\sigma_z}{2}\right)^2 + \tau_{xy}^2},$$

Where σ_1 and σ_3 are first (maximum) and third (minimum) principal stresses accordingly. For the purpose of calculating principal normal stresses, a conservative assumption is made that maximum shear stress τ_{xy} is acting over entire braze plane. Maximum principal shear stresses calculated as:

$$\tau_{max} = \frac{|\sigma_1 - \sigma_3|}{2}$$

First principal normal and maximum principal shear stresses calculated as described above are listed in Table 7 and plotted in Fig.14

References

1. Flom, Y., Wang, L., Powell, M. M., Soffa, M. A., and Rommel, M. L., Evaluating Margins of safety in Brazed Joints, *Welding Journal*, 88(10), p. 31-37, 2009
2. Flom, Y., Failure Assessment Diagram for Brazed 304 Stainless Steel Joints, NASA/TM-2011-215876, June 2011
3. C3.2M/C3.2:2008, Standard Method for Evaluating the Strength of Brazed Joints, American Welding Society, Miami, Fla.
4. Brazing Handbook, Fifth Edition, American Welding Society, Miami, Fla, 2007
5. Welding Kaiser Aluminum, First Edition, Kaiser Aluminum and Chemical Sales, Inc., Kaiser Center, Oakland, 1967
6. Dowling, N. E., Mechanical Behavior of Materials: Engineering Methods for Deformation, Fracture, and Fatigue, Prentice Hall Inc., New Jersey, 1993
7. Young, W. C., and Budynas, R. G., Roark's Formulas for Stress and Strain, Seventh Edition, McGraw-Hill, 2002

REPORT DOCUMENTATION PAGE

*Form Approved
OMB No. 0704-0188*

The public reporting burden for this collection of information is estimated to average 1 hour per response, including the time for reviewing instructions, searching existing data sources, gathering and maintaining the data needed, and completing and reviewing the collection of information. Send comments regarding this burden estimate or any other aspect of this collection of information, including suggestions for reducing this burden, to Department of Defense, Washington Headquarters Services, Directorate for Information Operations and Reports (0704-0188), 1215 Jefferson Davis Highway, Suite 1204, Arlington, VA 22202-4302. Respondents should be aware that notwithstanding any other provision of law, no person shall be subject to any penalty for failing to comply with a collection of information if it does not display a currently valid OMB control number.

PLEASE DO NOT RETURN YOUR FORM TO THE ABOVE ADDRESS.

1. REPORT DATE (DD-MM-YYYY) 26-10-2010			2. REPORT TYPE Technical Memorandum		3. DATES COVERED (From - To)	
4. TITLE AND SUBTITLE Failure Assessment Diagram for Titanium Brazed Joints				5a. CONTRACT NUMBER		
				5b. GRANT NUMBER		
				5c. PROGRAM ELEMENT NUMBER		
6. AUTHOR(S) Yury Flom, Justin S. Jones, Mollie M. Powell, and David F. Puckett				5d. PROJECT NUMBER		
				5e. TASK NUMBER		
				5f. WORK UNIT NUMBER		
7. PERFORMING ORGANIZATION NAME(S) AND ADDRESS(ES) Goddard Space Flight Center Greenbelt, MD 20771				8. PERFORMING ORGANIZATION REPORT NUMBER		
9. SPONSORING/MONITORING AGENCY NAME(S) AND ADDRESS(ES) National Aeronautics and Space Administration Washington, DC 20546-0001				10. SPONSORING/MONITOR'S ACRONYM(S) NASA/ GSFC		
				11. SPONSORING/MONITORING REPORT NUMBER NASA TM-2011-215882		
12. DISTRIBUTION/AVAILABILITY STATEMENT Unclassified-Unlimited, Subject Category: Report available from the NASA Center for Aerospace Information, 7115 Standard Drive, Hanover, MD 21076. (443)757-5802						
13. SUPPLEMENTARY NOTES						
14. ABSTRACT The interaction equation was used to predict failure in Ti-4V-6Al joints brazed with Al 1100 filler metal. The joints used in this study were geometrically similar to the joints in the brazed beryllium metering structure considered for the ATLAS telescope. This study confirmed that the interaction equation $R\sigma + Rt = 1$, where $R\sigma$ and Rt are normal and shear stress ratios, can be used as conservative lower bound estimate of the failure criterion in ATLAS brazed joints as well as for construction of the Failure Assessment Diagram (FAD).						
15. SUBJECT TERMS Brazing, Structural Analysis, Interaction Equations, Failure Assessment Diagrams, Titanium						
16. SECURITY CLASSIFICATION OF:			17. LIMITATION OF ABSTRACT Unclassified	18. NUMBER OF PAGES 24	19a. NAME OF RESPONSIBLE PERSON Yury Flom	
a. REPORT Unclassified	b. ABSTRACT Unclassified	c. THIS PAGE Unclassified			19b. TELEPHONE NUMBER (Include area code) (301) 286-3274	

